

## Analysis of uncertainties in MEMS and their influence on dynamic properties

T. UHL, A. MARTOWICZ, I. CODREANU, A. KLEPKA

*Department of Robotics and Mechatronics  
AGH University of Science and Technology  
al. Mickiewicza 30, 00-059 Kraków, Poland  
e-mails: tuhl@agh.edu.pl, adam.martowicz@agh.edu.pl,  
codreanu@agh.edu.pl, klepka@agh.edu.pl*

AN APPLICATION OF UNCERTAINTY ANALYSIS of microelectromechanical resonator is presented. A number of different uncertain parameters have been considered, connected both to geometric characteristics and material property. Sensitivity analysis has been carried out in order to study the influence of each input uncertain parameter on the chosen dynamic characteristics. The propagation of given uncertainties into the variation of studied output parameter has been evaluated by means of the Monte Carlo simulation, the vertex method and genetic algorithms. Finite element model of microresonator has been elaborated. It has taken into account the phenomenon of viscous damping coming from the presence of surrounding air as well as the influence of constant electrostatic field.

**Key words:** MEMS, microresonator, FE model, dynamic properties, sensitivity analysis, uncertainty analysis.

Copyright © 2009 by IPPT PAN

### Notations

- $A$  area; cross-sectional area; area of capacitor electrodes,
- $b$  thickness of comb drive finger,
- $B$  dimension of rectangular shape,
- $c$  damping coefficient,
- $\mathbf{C}_{\text{DAMPERS}}$  global damping matrix consisting of resultant damping coefficients which represent presence of surrounding air,
- $d$  thickness of air film; distance; gap between capacitor electrodes,
- $F$  force,
- $J_1$  first-order Bessel function,
- $k$  stiffness coefficient,
- $\mathbf{K}$  global stiffness matrix aggregated for mechanical part,
- $\mathbf{K}_{\text{SPRINGS}}$  matrix consisting of resultant stiffness coefficients which represent the presence of electrostatic field,
- $L$  dimension of rectangular shape,
- $\mathbf{M}$  global mass matrix,
- $n$  iteration index,
- $r$  characteristic dimension of the area of cross-section i.e. radius for a circular shape, a half of grater dimension for a rectangular shape, etc.,

- $\mathbf{u}$  vector of nodal displacements in FE model,
- $\dot{\mathbf{u}}$  vector of nodal velocities in FE model,
- $\ddot{\mathbf{u}}$  vector of nodal accelerations in FE model,
- $V$  voltage,
- $x$  displacement along axis  $x$ ,
- $\dot{x}$  velocity along axis  $x$ ,
- $x_0$  initial displacement along axis  $x$ ,
- $x, y$  axes of Cartesian coordinate system,
- $\beta$  auxiliary factor in calculation of squeeze-film damping,
- $\delta$  effective decay distance,
- $\varepsilon$  relative permittivity of air,
- $\varepsilon_0$  permittivity of vacuum,
- $\lambda$  acoustic wave length,
- $\mu$  kinematic viscosity,
- $\rho$  density,
- $\sigma$  standard deviation,
- $v$  speed of sound wave,
- $\omega$  circular frequency of vibration.

## 1. Introduction

MICROELECTROMECHANICAL SYSTEMS (MEMS) [1] compose a class of devices that utilize mechanical and electronic parts of microscale, mainly made of silicon material and integrated in one package. MEMS technology gives the opportunity to construct very small movable mechanical parts, e.g.: flexures, rotating joints, racks, gears, membranes and beams of size of microns that can be assembled into microdevices. Pure mechanical components, together with the electronic part contained in one functionally-closed unit, enable many applications in biology, chemistry, optics, measurement techniques etc. Most known and nowadays commercially available MEMS applications are: accelerometers, gyroscopes, microphones, pressure sensors, micropumps, optic signal switchers, signal filters, microreactors, etc. [1].

MEMS are usually manufactured with lithography-based techniques used during production of integrated circuits. Generally, there are two kinds of manufacturing techniques that are applied to MEMS: bulk and surface micromachining [1]. The first one consists in micromachining of a wafer made of monocrystalline silicon, e.g. etching in KOH. Second technique of MEMS fabrication, in turn, means microstructuring of layers, typically made of polysilicon. In this case MEMS is built by deposition layer by layer on a given substrate. Described technique allows for creating suspended structures easily.

Manufacturing processes of MEMS does not guarantee infinite repeatability of characteristics of subsequent items of microdevice [2, 3]. They differ, one from another, as their geometry and material properties are not the same. This fact should be taken into account while designing MEMS, to be able to predict more realistic ranges of variation of interesting properties which are crucial for device

performance. Therefore uncertainty analysis is performed, firstly to study separately the influence of introduced uncertainties on investigated characteristics, and secondly to predict overall uncertainty propagation [4]. First part of the uncertainty analysis, known also as sensitivity analysis, allows for distinguishing between influential and non-influential parameters and helps to neglect some of them to make the analysis easier and less time-consuming. In the paper, an application of uncertainty analysis carried out for the finite element (FE) model of MEMS microresonator has been described. As an object of the study, fundamental operational resonance frequency has been chosen since the knowledge of its scatter is important to assess the quality of microresonator. Selected material and geometry properties have been treated as uncertain and their influence on interesting characteristics have been of concern by means of sensitivity analysis and analysis of uncertainty propagation. As microsystems feature the necessity of taking into account multiphysics approach, in the model of microresonator the phenomena of air flow and electrostatic field have been considered.

## 2. Uncertainty analysis

Uncertainty analysis is carried out in order to assess the influence of identified uncertainties (input parameters of analysis) on studied characteristics (output parameters). In case of mechanical structures, both the physical item of device and the computer model can be used to obtain the value of output parameters, namely by measurement (experimental tests) or with results of computer simulations. The procedure present in uncertainty analysis includes the following steps:

- a) identification and modelling of uncertainties,
- b) elaboration, validation and parameterization of the model which describes the studied characteristics of mechanical system in terms of uncertainty parameters,
- c) sensitivity analysis,
- d) selection and application of the method used for assessment of uncertainty propagation,
- e) uncertainty propagation in characteristics of real prototypes, if possible, to perform verification of results for uncertainty propagation.

First task during the uncertainty analysis is establishment of the set of uncertain parameters which are taken into account. There is a well-known division of uncertainties that distinguishes: reducible uncertainty (also defined as epistemic, subjective uncertainty) and irreducible uncertainty (also known as variation, aleatory uncertainty) [5–7]. The first group arises from potential deficiency of knowledge on design parameters. Reducible uncertainty can be limited when the required information is gradually gathered. Common sources of such uncertainty are imprecision, inconsistency and lack of information. The examples are

different possible techniques of modelling of the same phenomenon, e.g. friction, damping. Irreducible uncertainties are substantially connected with modelled mechanical system and express inevitable variation of its properties within time, subsequent items, changes of environmental conditions etc. The examples are manufacturing tolerances. Uncertainties are present at all stages of life of a mechanical structure [5, 7]. Table 1 presents exemplary sources of uncertainties.

**Table 1. Uncertainties present at subsequent stages of life of mechanical structure**

Design	Manufacturing	Operation
<ul style="list-style-type: none"> <li>– choice of a solution concept</li> <li>– topology and number of structural elements</li> <li>– incomplete information on material properties</li> <li>– variety of methods for modelling physical phenomena</li> <li>– approximation, numerical errors</li> </ul>	<ul style="list-style-type: none"> <li>– change in quality of manufacturing of components and of the final product</li> <li>– differences in geometry due to manufacturing tolerances</li> <li>– wearing and aging of tools</li> <li>– imprecision of measuring devices</li> <li>– quality of joints</li> </ul>	<ul style="list-style-type: none"> <li>– changes of environmental conditions (temperature, humidity, pressure)</li> <li>– variable loading conditions</li> <li>– changes of properties due to aging, wearing and deterioration of original parameter values (corrosion, fatigue, microcracks)</li> </ul>

During modelling of uncertain parameters many factors should be taken into account. Usually, it happens that there is no equal access to complete data and their precision is problematic. Amongst all, the following factors determine the choice of uncertainty model:

- a) availability of information,
- b) knowledge of statistical moments/probability density functions (PDF),
- c) type of data: subjective/objective data, qualitative/quantitative judgment, linguistic variables,
- d) requested type of the output characteristics,
- e) dependences between uncertain parameters.

Depending on the format of gained data, uncertain parameters can be modelled as [5, 6, 8]: random variables or random fields (defined by means of statistical moments), intervals (defined with the extreme values of a parameter) and fuzzy numbers/fuzzy sets (stand for alternative of random variables and allow for linguistic definition of uncertain parameters i.e. representing subjective or incomplete knowledge).

The format of uncertainties determines the usage of applicable method for uncertainty analysis. Available methods for uncertainty analysis can be divided into the following categories [6, 8]:

- a) Probabilistic methods. They operate on random variables and random fields. They allow to find histograms and selected statistics characterizing

specific responses. The most commonly used method, among the probabilistic ones, is the Monte Carlo simulation (MCS). It can be used in the most basic form as a crude MCS and with some more sophisticated methods of sampling in parameter space, in order to reduce the required number of samples and to improve their locations in input domain.

- b) Possibilistic methods. They stand for major alternative for probabilistic methods. Most commonly used in the design stage when there is available only a limited knowledge on the PDF and statistics of the parameters. The most popular methods are: interval analysis [9], vertex method [6], theory of fuzzy sets with Zadeh's extension principle [10], transformation method and its modifications [11, 12].

In the paper, the results of uncertainty analysis have been obtained by the use of MCS for the study of histogram of the chosen resonance frequency. Additionally, the vertex method and genetic algorithms (GA) have been applied to search for extremes of the interesting characteristics.

### 3. FE model of microresonator

The variation of chosen resonance frequency of MEMS microresonator was of concern. Prediction of studied dynamic characteristics has been facilitated by computer simulations of numerical model, as it is normally done within the frame of virtual prototyping procedure [13]. To study the influence of assumed uncertainties on the output parameter, a FE model of microresonator has been elaborated. It is shown in Fig. 1.

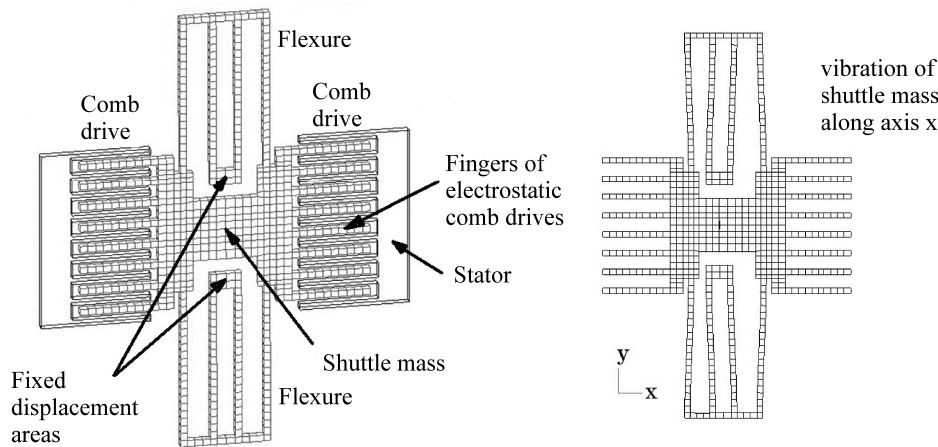


FIG. 1. FE model of microresonator and operational normal mode.

The FE model consists of a movable shuttle mass suspended over the substrate using two area-efficient folded flexures. Microresonator features two comb drives enabling both to activate the device and to measure the displacement along the longitudinal axis  $x$ . By mounted drives the microresonator can be externally actuated to vibrate with fundamental frequency of operation. The overall dimensions of the moving part of the device are  $288\ \mu\text{m}$  and  $186\ \mu\text{m}$ . The thickness of microresonator is  $3\ \mu\text{m}$ . The gap between the moving part and substrate is also  $3\ \mu\text{m}$ . The mesh is composed by 634 FE connected in 2072 nodes. The description of all structural elements is presented in Fig. 2.

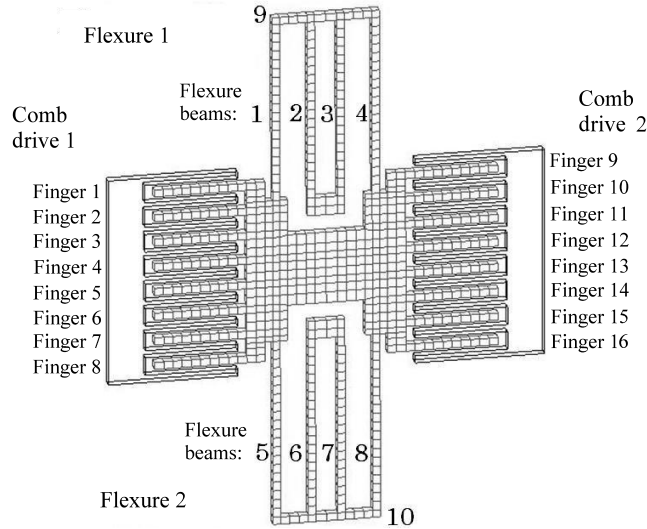


FIG. 2. Numbering of structural elements of the FE model of microresonator.

The considered normal mode stands for the third global mode, defined as the vibration of shuttle mass along axis  $x$  and presented in Fig. 1 on the right. The stability of resonance frequency related to the mentioned vibration mode is most important since it is activated while the microresonator is in operation in accelerometer or in the electric circuit applied for signal filtering. The value of resonance frequency calculated for nominal design equals  $137.0\ \text{Hz}$ . During calculation, the analysis of Modal Assurance Criterion (MAC) is performed every single iteration to prevent the results from confusion of the modes which may happen as the consequence of mode swapping phenomenon.

In the model, the presence of air damping and electrostatic field is considered. The mentioned phenomena are introduced in a simplified way, by addition of the discrete mechanical elements: dampers and springs. They express viscous damping of the surrounding air as well as approximate resultant stiffness of electrostatic influence and stand for an alternative to coupled problems [1]. Solved matrix equation of motion for FE model takes the form:

$$(3.1) \quad \mathbf{M}\ddot{\mathbf{u}} + \mathbf{C}_{\text{DAMPERS}}\dot{\mathbf{u}} + (\mathbf{K} + \mathbf{K}_{\text{SPRINGS}})\mathbf{u} = \mathbf{0},$$

where  $\mathbf{u}$  stands for nodal displacements,  $\mathbf{M}$ ,  $\mathbf{K}$  are global mass and stiffness matrices representing respectively pure mechanical parts of microresonator considered as an undamped system. Added parts consist of matrices  $\mathbf{C}_{\text{DAMPERS}}$  and  $\mathbf{K}_{\text{SPRINGS}}$  which introduce resultant damping and stiffness coefficients between the selected degrees of freedom. Considered approximation enables one-way coupling. Only the influence of air and electrostatic field on mechanical part is taken into account. The interaction of mechanical part on electrostatic field and flow of air has not been considered. Therefore there have not been introduced any additional degrees of freedom (DOF) describing the mentioned phenomena.

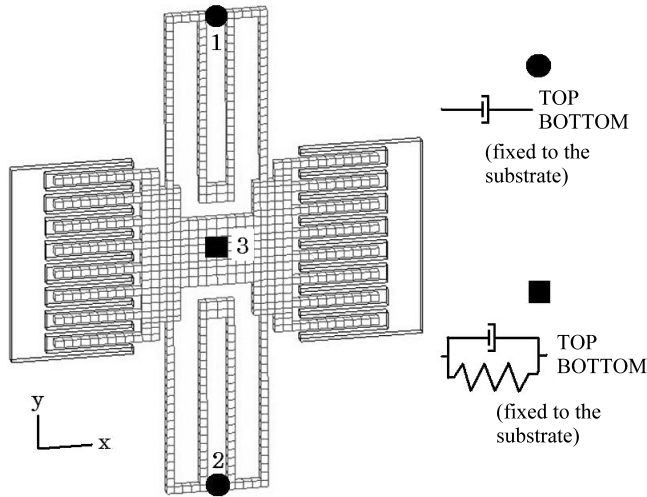


FIG. 3. Mechanical elements representing air damping and electrostatic field in numerical simulations.

Figure 3 presents localizations of introduced mechanical elements expressing the influence of air and electrostatic field. Six nodes have been chosen to which dampers and springs are connected. All of them are paired to represent both connections at top and bottom horizontal surfaces (in plane  $x$ - $y$ ). The localizations are as follows: 1 – in the middle of the flexure 1 for the introduction of air damping related to this part, 2 – the same purpose but for the flexure 2, 3 – in the middle of shuttle mass, for dampers introducing the influence of air on moving mass and springs that express the presence of electrostatic field generated by comb drives. Free element connections are fixed to the substrate. Summing up, 6 dampers and 2 springs are considered, acting only in the direction of fundamental operational resonance vibrations, i.e. along axis  $x$ . It has been assumed that

the influence of surrounding air and electrostatic field on other normal modes is skipped. Introduced elements have been modeled using PBUSH/CBUSH elements in MSC/Nastran. In the following two Sections 4 and 5, the introduction of air damping and electrostatic field is described.

It should be noted that in case of the presented model, i.e. when only one normal mode is studied, there is a possibility of further simplification considering the complexity of the model. As it is done in modal analysis, one normal mode can be represented by a simple one-DOF oscillator. This kind of simplicity enables the analyst to perform numerical simulation much quicker. However, the use of such model in the context of uncertainty analysis could be problematic. FE model takes some time to be simulated but also enables to consider all changes in geometry easily, e.g. via mesh morphing procedure, while in case of one-DOF system there is a necessity to calculate the resultant mass, stiffness and damping coefficients using very complicated, probably empirical, formulas. FE model guarantees that all geometric properties are accurately calculated with respect to geometric uncertainties.

#### 4. Air damping

There have been considered four different types of air damping in the model of microresonator, connected with: slide-film damping force (considered parallel movement of an object with respect to surrounding air; area of longitudinal cross-section is important), drag force (during movement through the air; area of transversal cross-section is important), squeeze-film damping force (when movement of an object against other element which is very closely located) and acoustic energy dissipation (activating acoustic waves spreading through air). Damping coefficients have been calculated separately for each damper, for given combination of the values of uncertain parameters.

In the model, two kinds of slide-film damping force have been introduced taking into account the difference between gap dimensions over and under the moving part of microresonator. Under the shuttle mass, where the dimension of gap distance equals  $3\ \mu\text{m}$ , Couette flow has been considered. Over the microresonator, the Stokes flow has been taken into account as the gap over the model has been assumed to be much greater than the effective decay distance  $\delta = 5.7\ \mu\text{m}$ , defined by the formula (4.3). In case of the sidewalls, both the Couette and Stokes flows have been considered, depending on the distance between model parts (Couette flow has been applied mainly between fingers of comb drives). Figure 4 shows the areas taken for the calculation of slide-film damping related to top and bottom surfaces of moving part. Mentioned areas are divided into 3 domains, each connected with different pairs of dampers (flexure 1: top and bottom, etc.).

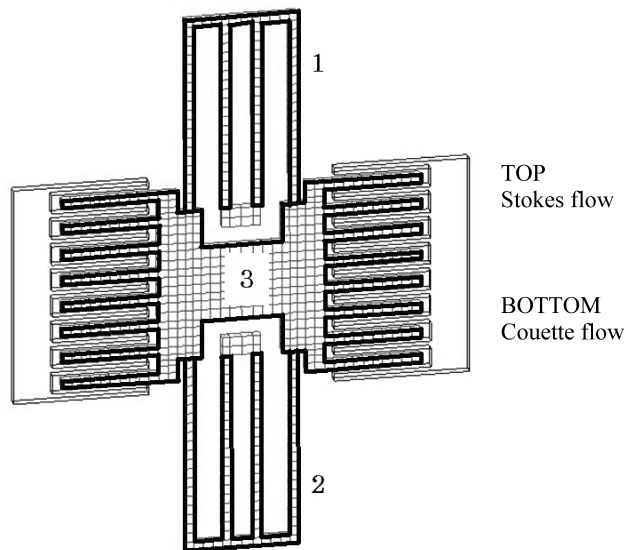


FIG. 4. Slide-film damping force; considered areas for bottom and top surfaces of moving part.

Both the Couette and Stokes flow have been taken into account while calculating slide-film damping of the sidewalls. The definition of flows for selected sidewalls is presented in Fig. 5.

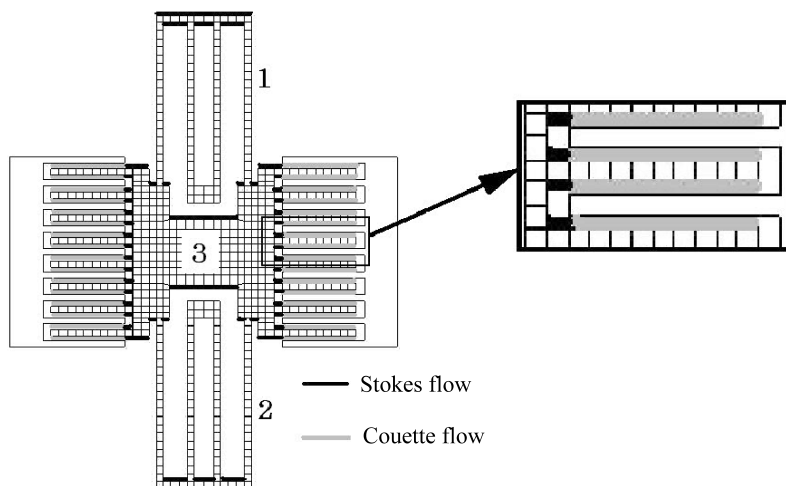


FIG. 5. Slide-film damping force; considered areas for sidewall surfaces of moving part.

The formulas presented below have been used to calculate damping coefficients  $c$ . Slide-film damping forces can be calculated using the following equations [14]:

- a) for Couette flow (when distance between the moving part and anchor/substrate is small, i.e. less than the effective decay distance  $\delta$ ):

$$(4.1) \quad F = \mu \frac{A}{d} \dot{x} = c\dot{x};$$

- b) for Stokes flow (when distance between the moving part and anchor/substrate is greater than effective decay distance  $\delta$ ):

$$(4.2) \quad F = \mu \frac{A}{\delta} \dot{x} = c\dot{x},$$

where:  $\mu$  is kinematic viscosity of fluid (for air it equals  $1.81 \cdot 10^{-5}$  Pa · s),  $A$  is the area of moving part at top or bottom of the microresonator,  $d$  is distance (thickness of air film),  $\dot{x}$  is velocity of shuttle mass along axis  $x$ ,  $c$  is the damping coefficient used to define the property of damper.

Effective decay distance  $\delta$  (in the model it equals  $5.7 \mu\text{m}$ ) is calculated as follows:

$$(4.3) \quad \delta = \sqrt{2\mu/\rho\omega},$$

where:  $\rho$  is fluid density (for air it equals  $1.2 \text{ kg/m}^3$ ),  $\omega$  is circular frequency of vibration.

Figure 6 presents all areas that have been taken into account to calculate damping coefficients representing the drag force, squeeze-film damping and dissipation via acoustic energy.

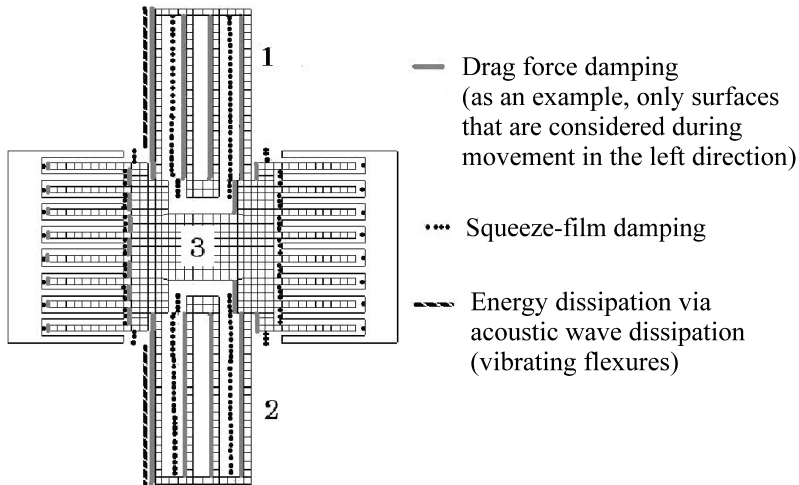


FIG. 6. Drag force, squeeze-film damping force and acoustic wave dissipation; considered areas for sidewall surfaces of the moving part.

To calculate the damping coefficient which represents the drag force the following formula has been used [14]:

$$(4.4) \quad F = \frac{32}{3} \mu r \dot{x} = c \dot{x},$$

where  $r$  is a characteristic dimension, which means a half of the greater dimension in case of rectangular shape of the object moving through air.

When distances between the neighbouring elements moving one against another are small, the squeeze-film damping should be considered. Mentioned damping expresses the phenomenon of under- or overpressure that occurs in case of small gaps. Squeeze-film damping force is calculated as follows:

$$(4.5) \quad F = \mu \frac{LB^3}{d^3} \beta \left( \frac{B}{L} \right) \dot{x} = c \dot{x},$$

where:  $L$ ,  $B$  are dimensions of rectangular shape ( $L > B$ ). Factor  $\beta(B/L)$  can be found by the formula [14]:

$$(4.6) \quad \beta \left( \frac{B}{L} \right) = \left\{ 1 - \frac{192}{\pi^5} \left( \frac{B}{L} \right) \sum_{n=1,3,5}^{\infty} \frac{1}{n^5} \operatorname{th} \left( \frac{n\pi L}{2B} \right) \right\}.$$

The last kind of damping which has been considered in the study is related to energy dissipation via acoustic waves. Each object vibrating in the fluid is a source of acoustic energy. Therefore the resistant damping force is observed and can be calculated from the following formula [14]:

$$(4.7) \quad F = \rho v A \left\{ 1 - 2J_1 \left( \frac{4\pi r}{\lambda} \right) \right\} / \left( \frac{4\pi r}{\lambda} \right) \dot{x},$$

where:  $v$  is speed of sound wave in the fluid (assumed as 343 m/s for air),  $\lambda$  is length of sound wave and  $J_1$  is the first order Bessel function.

Figure 7 presents the bar diagram of all damping coefficients calculated for nominal values of uncertain parameters.

While modeling viscous damping, slide-film damping and drag force are the most important phenomena and should be taken into account. Coefficients which represent squeeze-film and acoustic wave dissipation have values approximately 20 times smaller than the values of coefficients expressing slide-film and drag force. Therefore, they can be neglected for the analyzed model. Moreover it is seen that for the studied microresonator, clear division between all kinds of viscous damping can be made with respect to the part of model they mostly influ-

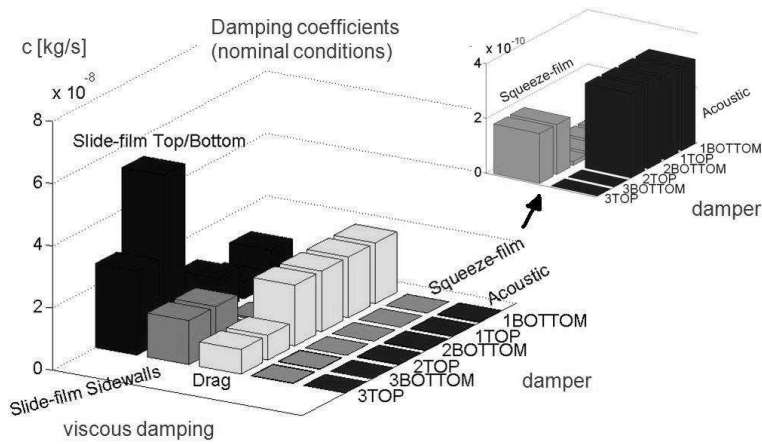


FIG. 7. Damping coefficients for nominal configuration.

ence on. Thus, slide-film damping and squeeze-film damping affect mostly shuttle mass, whereas drag force and acoustic dissipation influence mainly the flexures.

### 5. Electrostatic field

Since the comb drives can be treated as collection of capacitors in which normal and tangential forces act, in the studied case, both the mentioned forces have been used to model the influence of electrostatic field. Figure 8 symbolically defines all capacitors that have been taken into account, both being responsible for generating the tangential and normal forces.

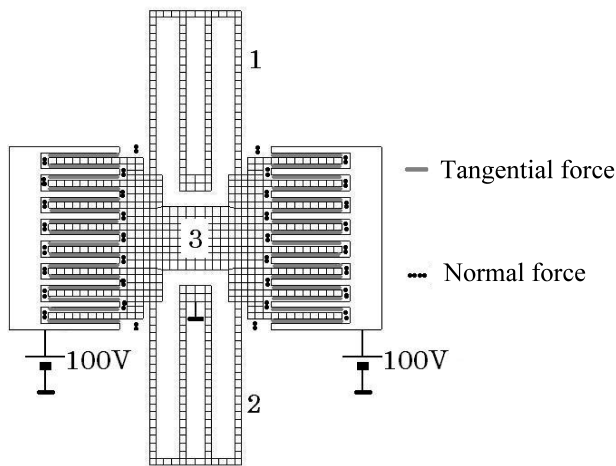


FIG. 8. Considered areas of capacitors and supplied voltage.

For the reason of simplicity, fringe effect has been neglected [14]. The presence of electrostatic field is considered by means of two springs, for which approximate stiffness coefficients have been calculated by the use of the following formulas defining:

a) tangential force:

$$(5.1) \quad F = \frac{b\varepsilon\varepsilon_0}{2d}V^2;$$

b) normal force:

$$(5.2) \quad F = \frac{A\varepsilon\varepsilon_0}{2}V^2\frac{1}{x^2} \approx \left(\frac{\partial F}{\partial x}\right)_{x=x_0} \cdot x = kx,$$

where:  $\varepsilon$  is the relative permittivity of air,  $\varepsilon_0$  is the permittivity of vacuum,  $V$  is voltage,  $b$  is thickness of comb drive finger,  $d$  is the gap between electrodes (gap between elements of comb drives that lie one in front of another and make horizontal and vertical capacitors),  $A$  is the area of electrodes of vertical capacitors,  $x$  and  $x_0$  are respectively displacement and initial displacement of shuttle mass along the x-axis.

Tangential forces, calculated for horizontal capacitors, do not depend on the displacement observed in considered mode of vibration. Hence, they are not taken into account in calculation of stiffness coefficients. Resultant tangential force is constant because the applied voltages do not change their values. Moreover, the voltages are symmetrical (each 100 V with the same polarization) and it has been assumed that all tangential forces cancel their influences on the behaviour of microresonator. For normal forces, resultant stiffness coefficient is calculated by the following formula, derived from Eq. (5.2):

$$(5.3) \quad k \approx \left(\frac{\partial F}{\partial x}\right)_{x=x_0} = -A\varepsilon\varepsilon_0V^2\frac{1}{x_0^3}.$$

Nominal value for resultant stiffness coefficient (the sum of stiffness coefficients calculated for bottom and top springs) equals  $-0.256$  N/m. To make the comparison, it should be noted that for nominal design, the resultant stiffness coefficient of two flexures (i.e. calculated in case when microresonator is considered as a single-DOF mechanical system elaborated only for the studied normal mode) and equals  $52.0$  N/m.

## 6. Uncertainties in FE model

63 different uncorrelated uncertain parameters have been of concern, expressing both the geometric and material properties of FE model of microresonator. Table 2 gives detailed information on uncertainty characteristics. All parameters

**Table 2. Uncertain parameters introduced in FE model of microresonator.**

No. of parameter	Description	Nominal value	Maximal range of variation
1–16	Finger length (comb drives, fingers 1–16)	50 $\mu\text{m}$	$\pm 0.5 \mu\text{m}$
17–32	Finger width (comb drives, fingers 1–16)	4 $\mu\text{m}$	$\pm 0.1 \mu\text{m}$
33–48	Finger y-axis shift (comb drives, fingers 1–16)	0 $\mu\text{m}$	$\pm 0.2 \mu\text{m}$
49–50	Flexure length (flexures 1, 2)	100 $\mu\text{m}$	$\pm 1 \mu\text{m}$
51–60	Width of flexure beams (flexure beams 1–10)	4 $\mu\text{m}$	$\pm 0.1 \mu\text{m}$
61	Resonator thickness	3 $\mu\text{m}$	$\pm 0.2 \mu\text{m}$
62	Chamfer angle of deposited layers (moving part)	0 deg	0–2 deg
63	Young's modulus of polysilicon	165 GPa	$\pm 3\%$ ( $\pm 5$ GPa)

have been modelled as intervals. In case of MCS (description in Sec. 8), normal PDF have been used considering that  $\pm 3\sigma$  corresponds to maximal range of variation (Table 2).

In this section, it should be noted that there is a number of different characteristics changes connected with the geometry and material used for MEMS construction. Some of them are catastrophic changes (i.e. faults, defects) which disable proper operation. Most known are [15]:

- a) not full release of a suspended microstructure,
- b) presence of unwanted oxide residuals, contaminants,
- c) re-deposition of etched material,
- d) break of supporting beams,
- e) sticktion of the parts as a result of adhesion forces and voltage overrange (pull-in effect),
- f) misalignment during etching and deposition,
- g) residual stress that causes the beam structures to deform.

The phenomena presented above are not included into the study unless they influence material and geometry properties shown in Table 2. Anyway they are not taken into account explicitly.

The described FE model has been parameterized with respect to introduced uncertainties. Fig. 9 presents the scheme of performed calculations that give the results of simulated model characteristics (frequency of operational vibration mode) for a given combination of input uncertain parameters. This model has been used for sensitivity analysis and to assess the uncertainty propagation.

Model updating done within each calculation loop consists of: calculation of all damping and stiffness coefficients which are used to parameterize dampers

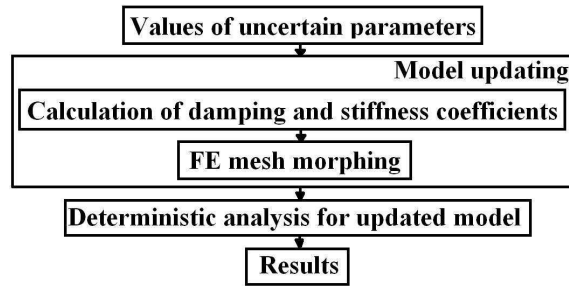


FIG. 9. The scheme of simulation loop.

and springs (presented in Fig. 3) and FE mesh morphing performed to change the geometry of the model.

## 7. Sensitivity analysis

Sensitivity analysis has been carried out in order to quantify the influences of all uncertain parameters on operational frequency of vibration. Finite difference method has been applied to approximate the first derivatives [16]. Central plan has been used for uncertainties apart from the chamfer angle, where forward plan has been applied. Figure 10 shows the results obtained in sensitivity analysis. All parameters are ordered according to numbering presented in Fig. 2.

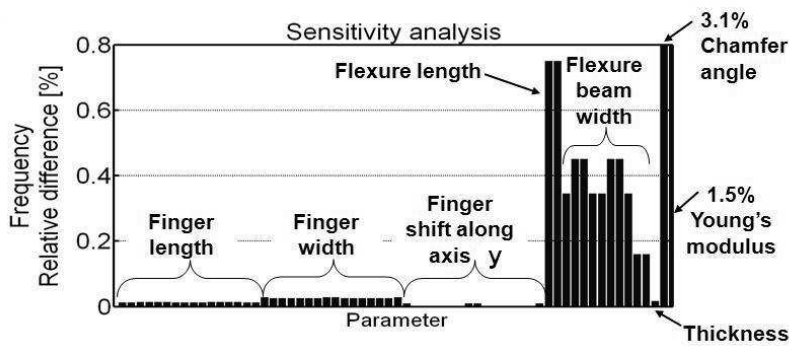


FIG. 10. Calculated sensitivities.

The most influential parameters are: chamfer angle, Young's modulus of polysilicon material and all 12 geometric characteristics describing flexures. Parameters presented above should be as first of engineers' concern while improving manufacturing process to keep variation of operational resonance frequency within required ranges. Thickness does not influence the interesting parameter significantly as it means the same scaling of stiffness and mass of moving part. Geometry of comb drive fingers and their shifts along axis  $y$  can be neglected because of their slight influence on the interesting natural frequency.

## 8. Uncertainty propagation

To perform the analysis of uncertainty propagation, the following methods have been applied:

- a) MCS. MCS has been used to find histograms of the studied parameter. Normal PDF have been considered with the assumption that  $-/+3\sigma$  intervals correspond to maximal ranges of variations (Table 2). Technique of Latin hypercube has been applied to improve the covering of input domain with generated samples [17]. Number of samples is 2500.
- b) The vertex method. The method has been used to search for the bounds of variation of the interesting frequency and means checking all the vertices of input domain that are considered as combinations of extreme values of input parameters. For the analysis, 14 most influential parameters have been chosen by sensitivity analysis (flexure lengths – 2 parameters, flexure widths – 10 parameters, chamfer angle and Young’s modulus of polysilicon) and 16384 iterations performed.
- c) The application of GA [18, 19]. GA have been used in order to find extremes of the chosen natural frequency. Therefore two search tasks have been performed. The first one for the search of minimal value and the second one to find the maximal value. Used population consists of 25 individuals that have been subjected to crossover and mutation procedures. The generation gap equals 0.8. 120 generations have been carried out in both tasks. Probabilities of crossover and mutation are equal 0.7 and 0.4 respectively.

Figure 11 presents histograms of selected damping coefficients obtained in MCS, namely for slide-film damping and acoustic energy dissipation. More de-

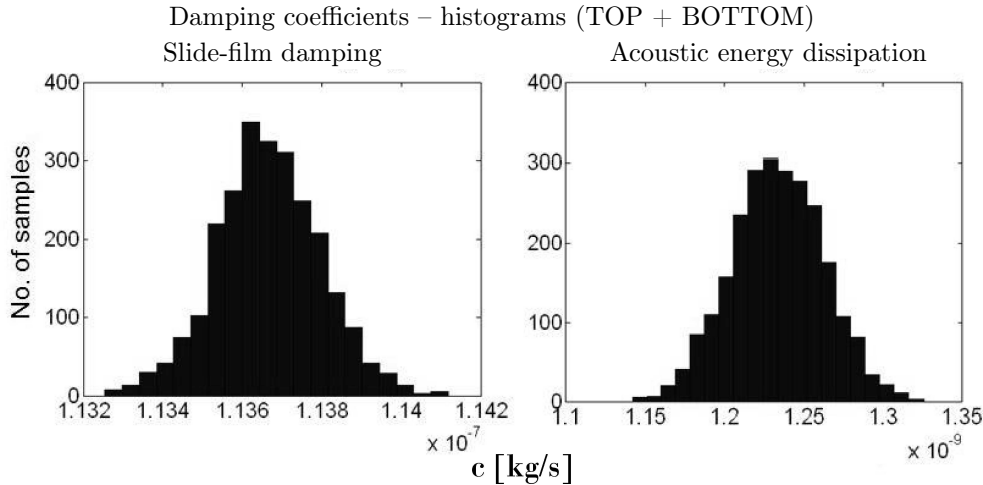


FIG. 11. Histograms of selected damping coefficients.

tailed information on all damping coefficients is shown in Table 3. It contains Coefficient of Variation (COV; known also as Coefficient of Variance [20]) as a reliable quantity used for the assessment of obtained scatters.

**Table 3. Damping coefficients – uncertainty propagation.**

Damping coefficients $c$ – sum for all dampers [ $10^{-10}$ kg/s]	Mean value	Standard deviation	COV [-]	Minimal value	Maximal value
				(relative change with respect to the mean value [%])	
Slide-film Top/Bottom	1136.7	0.1310	0.0012	1132.6 (-0.36)	1141.2 (0.40)
Slide-film Sidewalls	300.76	0.6695	0.0223	277.68 (-7.67)	324.15 (7.78)
Drag	938.30	0.1868	0.0020	931.08 (-0.77)	944.36 (0.65)
Squeeze-film	4.210	0.0258	0.0613	3.3822 (-19.7)	5.2075 (23.7)
Acoustic energy dissipation	12.336	0.0293	0.0238	11.415 (-7.47)	13.256 (7.46)

Although slide-films for the top and bottom surfaces of microresonator and drag characterize the highest values of damping coefficients, they seem to be the most insensitive in terms of the considered uncertainties. Calculated COV equal 0.12% and 0.20% respectively and are much smaller than the COV calculated for other damping coefficients. Amongst the three most influential damping coefficients, only that calculated for slide-film of sidewalls characterizes a considerable value of COV (2.23%) i.e. it is more sensitive to the assumed changes of design parameters. COV determined for the remaining damping coefficients, calculated for squeeze-film phenomenon and acoustic energy dissipation, are the highest ones, 6.13% and 2.38% respectively. However, their overall contribution to the sum of all damping coefficients equals 0.69%. Therefore we should not pay much attention to the accuracy of modelling of the mentioned phenomena.

Variation of the stiffness coefficient determined for MCS is described by the histogram presented in Fig. 12. Its numerical characteristics is collected in Table 4. The results of uncertainty propagation for operational frequency of vibration are presented in Fig. 13 and Table 5.

Results obtained by the applications of GA and by the vertex method are almost the same. Significant difference appears while comparing results yielded by MCS. MCS can be successfully applied to assess the selected statistics and histograms, but it is very time-consuming to use this method to perform reliable search for extremes of interesting characteristics. Even after the use of Latin

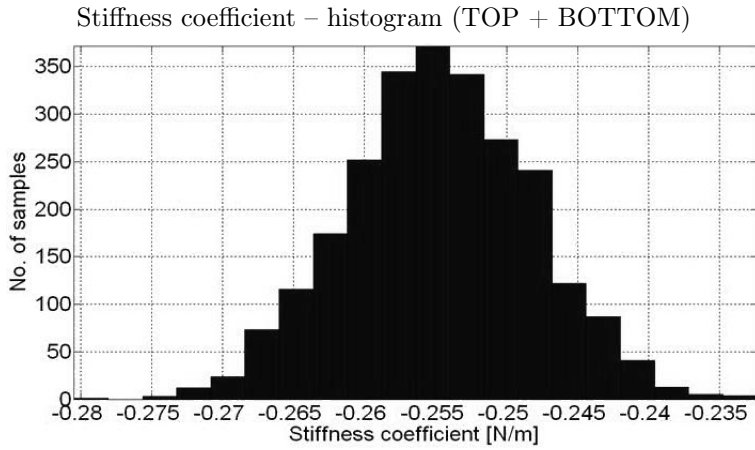


FIG. 12. Histogram of stiffness coefficient.

**Table 4. Stiffness coefficient – uncertainty propagation.**

Stiffness coefficient $k$ – sum for all springs [N/m]	Mean value	Standard deviation	COV [-]	Minimal value	Maximal value
	(relative change with respect to the mean value [%])				
	-0.2547	0.0066	-0.0257	-0.2804 (-9.53)	-0.2324 (9.22)

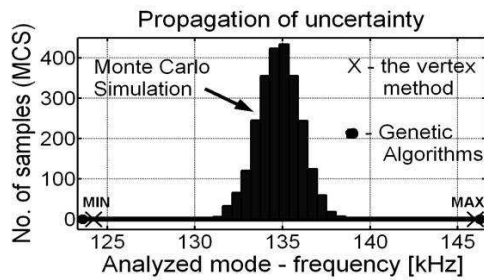


FIG. 13. Uncertainty propagation for studied frequency – graphical representation.

**Table 5. Uncertainty propagation for studied frequency – the case with 3% of variation of Young's modulus.**

Analysis	Resonance frequency [kHz]				
	Mean value	Standard deviation	COV [-]	Minimal value	Maximal value
MCS	134.79	$1.2114 \cdot 10^3$	0.0090	130.50	138.60
GA	–	–	–	123.60	146.26
Vertex	–	–	–	124.22	146.02

hypercube sampling techniques, the number of 2500 samples is not sufficient to cover properly the whole input parameter domain.

Although the originally assumed range of variation of Young's modulus equals  $\pm 3\%$  (i.e.  $\pm 5$  GPa; as presented in Table 2), additional analysis of uncertainty propagation has been performed to study the influence of scatter of the mentioned material property on the variation of the considered resonance frequency. Figure 14 and Table 6 present the results obtained in the analysis, both in the form of histograms and statistic characteristics.

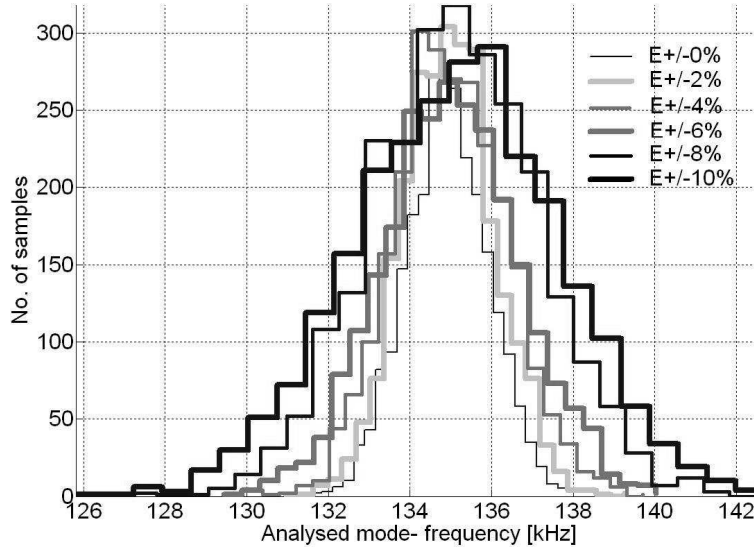


FIG. 14. Histograms of operational resonance frequency for different scatters of Young's modulus.

Table 6. Variation of studied frequency with respect to variation of Young's modulus.

Range of variation of Young's modulus [%]	Resonance frequency [kHz]				
	Mean value	Standard deviation	COV [-]	Minimal value	Maximal value
				(relative change with respect to the mean value [%])	
0	134.79	$1.007 \cdot 10^3$	0.0075	1.314 (-2.486)	1.380 (2.399)
2	134.80	$1.114 \cdot 10^3$	0.0083	1.308 (-2.984)	1.394 (3.443)
4	134.79	$1.369 \cdot 10^3$	0.0102	1.300 (-3.711)	1.399 (3.803)
6	134.79	$1.671 \cdot 10^3$	0.0124	1.292 (-4.135)	1.403 (4.053)
8	134.78	$2.056 \cdot 10^3$	0.0153	1.268 (-5.896)	1.428 (5.948)
10	134.78	$2.503 \cdot 10^3$	0.0186	1.255 (-6.902)	1.430 (6.130)

For the analysis, all geometric parameters can vary within the bounds defined in Table 2. Studied domain of material property covers ranges up to  $\pm 10\%$  of nominal value of Young's modulus. Approximately linear relationship between the range of variation of Young's modulus and COV calculated for the studied frequency is observed. COV increases twice when the range of variation of Young's modulus grows from 0% to 8%. Calculated mean values of resonance frequency are almost the same (from 134.78 kHz up to 134.80 kHz), however they significantly differ from the nominal value of this parameter (137 kHz). This observation can be explained by linear relationship between the studied frequency and Young's modulus and simultaneous strongly nonlinear relationships between this frequency and geometric parameters.

## 9. Summary and concluding remarks

In the paper an application of uncertainty analysis is presented on the example of simulation of dynamic properties of microresonator. As an object of the study, i.e. the output parameter of the analysis, a chosen resonance frequency of operational mode has been selected and its variation in terms of the assumed uncertainties has been assessed. Selected geometric parameters and material property have been considered as uncertain.

FE model of microresonator has been elaborated and parameterized with respect to the established list of uncertain parameters. The model has taken into account multiphysics. The influence of air damping and electrostatic field has been modeled by the use of discrete mechanical elements: dampers and springs. The following phenomena connected with air damping have been of concern: slide-film damping, drag force, squeeze-film damping and dissipation of acoustic energy. FE model has been used in sensitivity analysis and to assess the uncertainty propagation. Performed analysis has shown that acoustic energy dissipation and squeeze-film damping can be neglected for the studied device.

Amongst all geometric parameters, flexure characteristics and chamfer angle are most important for variation of the studied resonance frequency. It is so since stiffness of the structure vibrating in operational mode depends mostly on flexure geometry. Geometry of comb drive fingers can be skipped, since its changes slightly participate in variation of the output parameter. Thickness of the microresonator can be neglected because of small effect of this parameter on the studied frequency.

Different methods, both probabilistic and possibilistic, have been applied in order to study the uncertainty propagation for interesting natural frequency, namely: MCS, the application of GA and the vertex method. The first one has been used to obtain mean values and histograms of the output parameter. Remaining two methods have been used to calculate the extreme values of natural

frequency. The results obtained by the applications of the vertex method and GA are consistent. Minimal and maximal values yielded in MCS are different since the number of samples is supposed to be insignificant and covering of area of low probability seems to be of poor quality. During the analysis, linear relationship between operational resonance frequency and elastic modulus has been found as well as the nonlinear ones between the output parameter and the geometry characteristics of FE model of microresonator.

## Acknowledgments

The work was supported by the Polish Grant No. N N503 141236, entitled „Metoda wielokryterialnej optymalizacji konstrukcji mikroukładów z uwzględnieniem niepewności technologicznych” (“*The method of multiobjective optimization of the construction of micro-devices considering technological uncertainties*”).

## References

1. R.M. LIN, W.J. WANG, *Structural dynamics of microsystems – current state of research and future directions*, Mechanical Systems and Signal Processing, **20**, 1015–1043, 2006.
2. M. LIU, K. MAUTE, D.M. FRANGOPOL, *Multi-objective design optimization of electrostatically actuated microbeam resonators with and without parameter uncertainty*, Reliability Engineering and System Safety, **92**, 1333–1343, 2007.
3. A. MAWARDI, R. PITCHUMANI, *Design of microresonators under uncertainty*, Journal of Microelectromechanical Systems, **14**, 1, 63–69, 2005.
4. I. CODREANU, A. MARTOWICZ, A. GALLINA, L. PIECZONKA, T. UHL, *Study of the effect of process induced uncertainties on the performance of a micro-comb resonator*, Proc. of 4th Conference Mechatronic Systems and Materials 2008 – MSM 2008, Białystok, Poland, July 14–17, 2008.
5. D. MOENS, D. VANDEPITTE, *A survey of non-probabilistic uncertainty treatment in finite element analysis*, Computer Methods in Applied Mechanics and Engineering, **194**, 1527–1555, 2005.
6. D. MOENS, D. VANDEPITTE, *Non-probabilistic approaches for non-deterministic FE analysis of imprecisely defined structures*. Proc. of the International Conference on Noise and Vibration Engineering ISMA 2004, Leuven, Belgium, 3095–3119, September 20–22, 2004.
7. W.L. OBERKAMPF, S.M. DELAND, B.M. RUTHERFORD, K.V. DIEGERT, K.F. ALVIN, *Error and uncertainty in modeling and simulation*, Reliability Engineering and System Safety, **75**, 333–357, 2002.
8. G.I. SCHUELLER, *A state-of-the-art report on computational stochastic mechanics*, Probabilistic Engineering Mechanics, **12**, 4, 197–321, 1997.
9. R.E. MOORE, *Interval analysis*, Prentice-Hall, Englewood Cliffs, N.J. 1966.
10. D. DUBOIS, H. PRADE, *Fuzzy sets and systems. Theory and applications*, Academic Press, New York 1980.

11. M. HANSS, *Applied fuzzy arithmetic. An introduction with engineering applications*, Springer-Verlag, Berlin 2005.
12. M. HANSS, *The transformation method for the simulation and analysis of systems with uncertain parameters*, Fuzzy Sets and Systems, **130**, 277–289, 2002.
13. H. VAN DER AUWERAER, *Requirements and opportunities for structural testing in view of hybrid and virtual modeling*, Proc. of the International Conference on Noise and Vibration Engineering ISMA 2002, Leuven, 1687–1702, September 16–18, 2002.
14. M. BAO, *Analysis and design principles of MEMS devices*, Elsevier Science, 2005.
15. S. MIR, B. CHARLOT, B. COURTOIS, *Extending fault-based testing to micromechanical systems*, Journal of Electronic Testing: Theory and Applications, **16**, 279–288, 2000.
16. M. KLEIBER, H. ANTUNEZ, T.D. HIEN, P. KOWALCZYK, *Parameter sensitivity in non-linear mechanics*, John Wiley & Sons, Chichester, England 1997.
17. J.C. HELTON, F.J. DAVIS, *Latin hypercube sampling and the propagation of uncertainty in analyses of complex systems*, Reliability Engineering and System Safety, **81**, 1, 23–69, 2003.
18. D.E. GOLDBERG, *Genetic algorithms in search, optimization, and machine learning*, Addison-Wesley Publishing Company, Reading, Massachusetts, U.S.A., 1989.
19. Z. MICHALEWICZ, *Genetic algorithms + data structures = evolution programs*, Springer-Verlag, Berlin, Heidelberg 1996.
20. A. MAWARDI, R. PITCHUMANI, *Numerical simulations of an optical fiber drawing process under uncertainty*, Journal of Lightwave Technology, **26**, 5, 580–587, 2008.

Received July 30, 2008; revised version May 7, 2009.

---